International Journal of Food Microbiology 462 (2027) 112066

Contents lists available at ScienceDirect

International Journal of Food Microbiology

journal homepage: www.elsevier.com/locate/ijfoodmicro

Microbial variation and shelf life of chicken breast fillets: A year-long study across two European producers

Birgitte Moen [a,*], Beatriz Nunes Silva [b], Ingrid Måge [a], Paula Teixeira [b], Solveig Langsrud [a], Ingunn Berget [a], Merete Rusås Jensen [a], Mari Øvrum Gaarder [a], Ina Aksnes Lian [c], Dina Fernandes [d], Solfrid Bjørkøy [c], Diogo Ferreira [d], Annette Fagerlund [a]

[a] Nofima – Norwegian Institute of Food, Fisheries and Aquaculture Research, 1433 Ås, Norway
[b] Universidade Católica Portuguesa, CBQF – Centro de Biotecnologia e Química Fina – Laboratório Associado, Escola Superior de Biotecnologia, Rua Diogo Botelho 1327, 4169-005 Porto, Portugal
[c] Norsk Kylling AS, Havneveien 43, 7300 Orkanger, Norway
[d] Lusiaves – Indústria e Comércio Agro-Alimentar, S.A., Zona Industrial da ZICOFA Lote 4, Rua Cova das Faias, 2415-314 Leiria, Portugal

ARTICLE INFO

Keywords:
Spoilage microbiota
Sensory quality
Lag phase
Shelf-life prediction

ABSTRACT

Despite extensive research on poultry spoilage, variability across batches, seasons, and facilities remains poorly resolved, limiting evaluation of microbiological data for adaptive, data-driven shelf-life determination. This study examined whether initial microbial status, growth dynamics, microbiota composition, and sensory changes varied systematically over one year in modified atmosphere-packed (MAP) chicken breast fillets from two European producers using different gas compositions (Producer A, Norway; Producer B, Portugal). Fillets were analysed after production and during storage at 4 °C or under a 4 to 8 °C temperature shift. Initial total viable counts (TVC) were lower in fillets from Producer A than B, but both producers showed approximately 2-log variation between batches. Maximum growth rates were similar, but Producer B showed shorter model-derived lag times and reached 7 $\log_{10}$ CFU/g earlier. Within each producer, model-based time to 7 $\log_{10}$ CFU/g tracked most strongly with the model-derived lag parameter, whereas initial aerobic TVC showed limited association. During late storage, microbiota communities converged towards distinct spoilage profiles in products from the two producers, and these profiles were largely stable across production days (A: *Lactobacillales*, *Hafnia-Obesumbacterium*; B: *Brochothrix*, *Yersiniaceae*). Sensory deterioration correlated with TVC and was accelerated but not qualitatively altered by elevated temperature. Overall, initial aerobic TVC was not a reliable predictor of batch-specific shelf life under the MAP conditions studied. Instead, early follow-up measurements after a few days of storage may be needed to capture spoilage-community development and infer batch-specific early growth dynamics, although such indicators require further validation before practical implementation.

1. Introduction

Poultry meat, particularly chicken, remains one of the most consumed animal proteins in Europe due to its affordability, nutritional profile, perceived sustainability advantages relative to other meats, and broad consumer acceptance. In 2024, the EU produced an estimated 14.1 million tons of poultry meat, and the production is projected to grow by about 1 million tons over the period 2025–2035 (EC, 2025; Eurostat, 2025). However, chicken products are highly perishable and susceptible to microbial spoilage, which contributes to economic losses, food waste, and consumer dissatisfaction, and they may also carry foodborne pathogens relevant to foodborne outbreaks.

The microbial composition of chicken meat is shaped by multiple factors, including the animal's microbiota and farm environment, transport and pre-slaughter conditions, slaughter and processing environment and practices, seasonal variation, and post-processing factors such as cutting/handling, as well as storage temperature (Rouger et al., 2017; Sequino et al., 2025). Spoilage organisms commonly associated with poultry meat include *Pseudomonas* spp., *Enterobacteriaceae*, *Brochothrix thermosphacta* and lactic acid bacteria (LAB), mainly *Lactobacillus* spp. (sensu lato; including taxa reclassified, e.g. *Latilactobacillus*), *Carnobacterium* spp., *Leuconostoc* spp. and *Lactococcus* spp. (Herbert

* Corresponding author.
E-mail address: birgitte.moen@nofima.no (B. Moen).

https://doi.org/10.1016/j.ijfoodmicro.2026.112066
Received 22 May 2026; Received in revised form 21 August 2026; Accepted 10 September 2026
Available online 11 September 2026

et al., 2015; Lauritsen et al., 2019; Lee et al., 2017; Morales et al., 2016; Sequino et al., 2025). Other taxa, including *Photobacterium* spp., have also been isolated from spoiled poultry meat. Such findings may partly reflect differences in analytical approach, including culture-independent sequencing or media conditions that favour detection of specific bacterial groups, and highlight that reported spoilage communities can vary with methodology as well as product and storage conditions (Chen et al., 2020; Dourou et al., 2021; Sequino et al., 2025). The packaging atmosphere also affects microbial succession during storage by inhibiting some members of the initial microbiota while favouring the survival and growth of bacteria better adapted to the package environment (Kandeepan and Tahseen, 2022). Under aerobic conditions, the shelf life is typically shorter (five to six days), and modified atmosphere packaging (MAP) is therefore commonly used to extend it (Holck et al., 2014; Jimenez et al., 1997; Kandeepan and Tahseen, 2022).

MAP with elevated CO_2 concentrations suppresses aerobic spoilage organisms (e.g. *Pseudomonas* spp.) and promotes CO_2-tolerant facultative anaerobes, including LAB and *B. thermosphacta* (Holck et al., 2014; Marmion et al., 2021). Under MAP conditions, the relationship between initial aerobic total viable counts (TVC) and subsequent spoilage development may be less direct, as initial counts include both spoilage-associated bacteria capable of growing under the package conditions and background bacteria that may subsequently be inhibited. During storage, the relative contribution of bacteria selected by the MAP conditions increases, and the microbial composition underlying the total counts may therefore change over time. In such systems, spoilage is not solely determined by microbial load, but also by the metabolic activity and interactions of specific spoilage organisms (SSOs) within the microbial community (Hansen et al., 2023; Shao et al., 2021). Nevertheless, TVC is still commonly used as an indicator of microbiological acceptability, with a frequently applied threshold of 7 $\log_{10}$ CFU/g (Höll et al., 2016; Zhang et al., 2012). Noticeable odour changes are typically reported when TVC exceeds 8 $\log_{10}$ CFU/g (Naveena et al., 2017; Rouger et al., 2018; Wang et al., 2016), although certain species may cause spoilage at lower levels (Marmion et al., 2021). Sensory evaluation is therefore essential to link microbial dynamics with perceived spoilage and to establish meaningful shelf-life endpoints.

Food waste can result from a mismatch between a product's actual shelf life under real storage conditions and the shelf life declared through date marking, which may contribute to premature disposal. Notably, the European Commission's market study on date marking estimates that up to 10% of the 88 million tonnes of food waste generated annually in the EU are linked to date marking practices (ICF et al., 2018). While producers cannot control storage conditions throughout the supply chain, including transport and retail, restaurant, catering, distributor, or consumer, they may be able to reduce unnecessary waste by adjusting the use-by-dates to reflect batch-to-batch variability. Such adjustments would require predictive models that incorporate realistic cold-chain variation, including moderate temperature abuse scenarios, rather than relying only on ideal storage conditions. However, despite extensive research on spoilage microbiota composition and packaging technologies, there is still limited understanding of how spoilage varies across batches, seasons and facilities. To date, most shelf-life studies have focused on the effects of different temperatures or packaging concepts and have typically been based on a single or a limited number of batches. This knowledge gap poses a challenge for evaluating the feasibility of adaptive, data-driven shelf-life labelling, a concept where shelf life is predicted and the date mark is adjusted based on available information about each unit or batch, rather than fixed durations. Such information can derive from batch-specific characteristics at production (e.g., initial TVC, microbiota, pH, atmosphere) and/or from time-temperature exposure recorded along the supply chain (e.g., time-temperature indicator or time–temperature dependent loggers) (Li and Wang, 2017). Adaptive labelling is only feasible when shelf life is predictably related to these factors and when the resulting effect sizes are large enough to justify changes in labelling decisions (i.e., beyond measurement noise and consumer-handling variability). Under these circumstances, shelf life may be estimated using a spectrum of modelling approaches, ranging from predictive microbiology (growth/inactivation kinetics and temperature dependence), to statistical frameworks (e.g., regression, survival analysis, mixed-effects to capture producer/batch/day), and, where warranted by complexity, machine-learning approaches (Tarlak, 2023). If real-time prediction is not feasible, a potential pragmatic alternative is to adjust date marking by seasonal or within-day patterns (e.g., different shifts), provided these patterns are stable and validated.

To address the current knowledge gap, this study evaluated whether batch-to-batch variation in bacterial load, microbiota composition, and storage growth dynamics in MAP-packaged chicken breast fillets is sufficiently structured and predictable to inform adaptive, data-driven shelf-life decision-making. The primary aim was not to compare the two producers directly, but to assess whether microbial variation and shelf-life development were systematically structured over time within each producer. Data were collected over one year from two producers. Three parallel hypotheses were formulated: 1) Production day is associated with systematic and predictable variation in initial microbial status, microbiota composition and subsequent shelf-life development over the course of a year (production-day effects); 2) Batches produced at different times within the same production day differ systematically and predictably in initial microbial status, microbiota composition and subsequent shelf-life development (within-day batch effects); and 3) Higher initial TVC systematically predicts shorter time to sensory spoilage and/or a shorter time to reach 7 $\log_{10}$ CFU/g (initial-load effects). Evidence supporting these primary hypotheses would indicate that the corresponding factors could potentially be exploited to inform adaptive, data-driven shelf-life decisions; conversely, negligible, inconsistent, or poorly predictable differences would challenge the feasibility of adaptive shelf-life determination.

To test these hypotheses, packaged chicken breast fillets were collected from different production batches from two geographically distinct producers using different MAP gas compositions: one in Norway (Producer A) and one in Portugal (Producer B). Shelf-life studies were then conducted beyond the use-by date under two temperature scenarios (**stable** 4 °C and a temperature **shift** from 4 to 8 °C) to assess microbial and sensory changes during extended storage. Sampling was performed over one year, and for each production day, two batches originating from different chicken flocks were collected. Because the two producers used different MAP gas compositions, between-producer differences were interpreted descriptively; causal separation of producer and MAP effects would require a controlled packaging-atmosphere design.

2. Materials and methods

Samples were consumer packages of boneless, skinless chicken breast fillets (Pectoralis major and Pectoralis minor muscles), obtained

Table 1
Producer- and packaging-level parameters.

	Producer A	Producer B
Country	Norway	Portugal
No chickens processed daily	60,000–90,000	190,000
No shifts	1	2
Chicken breed	Hubbard	Ross Cobb
MAP gas	50–55% CO_2, 45–50% N_2	55–70% O_2, 20–30% CO_2, balance N_2
Packaging material	PET/PE	PET/PE
Package size (g)	1000 g ± 15–20 g[a]	459–809 g (average 653 g)
No fillets per package	4–5[b]	3–5
Shelf life (days)	20	7

[a] Allowable overfill of up to 20 g and underfill of up to 15 g.
[b] Occasionally 3 large fillets.

from two poultry producers (Producer A and Producer B; Table 1). Hereafter, these samples are referred to as "chicken fillets" or "fillets". The MAP of Producer A is termed high-CO_2 MAP, and the MAP of Producer B high-O_2 MAP.

2.1. Experimental design

From February to December 2024, consumer packages of chicken fillets packed on the slaughter day (day 0) were collected on seven production days distributed across the year (production days 1–7) (Table 2). In addition, chicken fillets from Producer A were included in a pilot shelf-life experiment in November 2023, which was designated production day 0. On each production day, two different flocks of chicken were sampled: the first ("early") and the last or next to last ("late") flock processed in the shift. For the pilot shelf-life experiment, only products from the early flock were analysed. For Producer A, the slaughter day was either Tuesday (A0, A1, A2, A3 and A7) or Thursday (A4, A5, and A6) and for Producer B, all sampled production days were Fridays.

Table 2
Overview of the sampling design for Producers A and B, including production day, slaughter and packaging date, storage temperature, time of day (early or late batch), storage and sampling days, and total number (N) of packages analysed for each scenario.

Prod.	Prod. day	Date	Temp.	Early	Late	Sampling days	N
A	0	31.10.2023	4 °C	✓		1, 7, 15, 17, 20, 22, 23, 27, 30	27
A	0		8 °C	✓		15, 17, 20, 23	12
A	1	20.02.2024	4 °C	✓	✓	1, 17, 20, 22, 24, 27	36
A	1		8 °C	✓	✓	17, 20, 22, 24	24
A	2	14.05.2024	4 °C	✓	✓	1, 7, 20, 24, 27	30
A	2		8 °C	✓	✓	10, 14, 17, 20	24
A	3	21.05.2024	4 °C	✓	✓	1, 7, 20, 24, 27	30
A	3		8 °C	✓	✓	10, 14, 17, 20	24
A	4	29.08.2024	4 °C	✓	✓	1, 7, 20, 25, 27	30
A	4		8 °C	✓	✓	15, 18, 20	18
A	5	12.09.2024	4 °C	✓	✓	1, 7, 18, 20, 25, 27	33
A	5		8 °C	✓	✓	15, 18, 20, 23	21
A	6	07.11.2024	4 °C	✓	✓	1, 7, 15, 18, 20, 25, 27	37
A	6		8 °C	✓	✓	11, 15, 18, 20	22
A	7	12.11.2024	4 °C	✓	✓	1, 7, 15, 17, 20, 24, 27	38
A	7		8 °C	✓	✓	10, 15, 17, 20	22
B	1	23.02.2024	4 °C	✓	✓	0, 7, 10, 12, 14, 17	33
B	1		8 °C	✓	✓	7, 10, 12, 14	24
B	2	31.05.2024	4 °C	✓	✓	0, 5, 7, 11, 14, 17	32
B	2		8 °C	✓	✓	4, 7, 11	16
B	3	14.06.2024	4 °C	✓	✓	0, 5, 7, 11, 14, 17	36
B	3		8 °C	✓	✓	4, 7, 11	18
B	4	05.07.2024	4 °C	✓[a]	✓	0, 5, 7, 11, 14, 17	21
B	4		8 °C		✓	5, 7, 11	9
B	5	12.07.2024	4 °C	✓	✓	0, 5, 7, 11, 14, 17	36
B	5		8 °C	✓	✓	4, 7, 11	18
B	6	20.09.2024	4 °C	✓	✓	0, 5, 7, 11, 14, 17	36
B	6		8 °C	✓	✓	4, 7, 11	18
B	7[b]	04.10.2024	4 °C	✓	✓	0	6

Abbreviations: Prod., producer; Prod. day, production day; Date, slaughter and packaging date; Temp., storage temperature; N, number of packages analysed. Early and late indicate batches sampled from the first and last/next-to-last flock processed during the shift, respectively.

[a] Only sampling day 0 samples from early batch were analysed.

[b] Due to a packaging error at this production day, only fresh (Day 0) samples could be analysed, as the products could not be stored for subsequent shelf-life analyses.

2.2. Storage conditions and sampling in the shelf-life study

The packages were transported to the research labs at 4 °C with overnight delivery (Producer A) or same-day delivery (Producer B). Two storage scenarios were used: stable storage at 4 °C (**stable** 4 °C) and a temperature-shift scenario from 4 °C to 8 °C (**shift** from 4 °C to 8 °C). For both scenarios, products were initially stored at 4 °C until day 3 (Producer B) or day 7 (Producer A). In the temperature-shift scenario, half of the packages were moved to 8 °C, simulating moderate temperature abuse during retail and consumer stages of the food chain during the last two-thirds of the declared product shelf life. The remaining packages were kept at 4 °C throughout storage.

Three replicate packages were sampled for each production batch and sampling point. Packages were sampled on the day of arrival, corresponding to day 1 for Producer A and day 0 for Producer B. Additional sampling was performed during storage at predefined time points (Table 2). In total, 731 packages were analysed from the two producers.

2.3. MAP gas analysis

To ensure the integrity of the MAP and to detect any potential gas leakage or incorrect gas composition, headspace concentrations of CO_2 and O_2 in the chicken packages were analysed using a Dansensor CheckMate 9900 or CheckMate 3 headspace gas analyser (Ametek Mocon, Denmark) with accuracies of $\pm 0.01\%$ O_2 and $\leq \pm 0.8\%$ CO_2. Predefined exclusion criteria were applied to remove packages with headspace values indicative of compromised MAP conditions. For Producer A, packages with $O_2 > 1\%$ were considered non-compliant and excluded, with one day-1 package retained despite elevated O_2 because microbial growth was assumed to be unaffected at this early stage. For Producer B, packages with both $O_2 < 25\%$ and $CO_2 < 15\%$ were considered indicative of loss of package integrity and excluded. All gas measurements are listed in Supplementary Table 1.

2.4. Microbiological enumeration

Two fillets from each package were placed in a sterile stomacher bag with filter, weighed, and 150 mL of peptone water (0.1% peptone, 0.85% NaCl; Oxoid, UK) was added. The contents were hand-massaged for 1 min. For packages containing large fillets, a single fillet was used, weighed and 100 mL of peptone water added.

To determine TVC and obtain colonies for MALDI-TOF MS identification, serial dilutions of the bag homogenates were prepared in peptone water and plated on standard plate count agar (PCA; Oxoid). Plates were incubated aerobically at 15 °C for 5–7 days to ensure recovery of psychotrophic spoilage organisms. In addition to aerobic PCA incubation, counts under product-like MAP conditions were assessed for initial samples from Producer A (storage day 1) throughout the study. For this analysis, inoculated PCA plates were placed in plastic trays comparable to those used for the chicken products and packed under the corresponding product MAP atmosphere. The MAP-incubated plates were stored at 15 °C for 10 days before enumeration. For Producer B, counts under product-like MAP conditions were assessed during the first production round (B1), but this additional enumeration was not continued in subsequent production rounds.

All TVC results are reported as $\log_{10}$ CFU/g and listed in Supplementary Table 1.

2.5. MALDI-TOF MS colony identification

To further investigate the dominant microbiota, bacterial isolates were identified by MALDI-TOF MS following a common analytical

framework applied by both the Norwegian and Portuguese teams, with minor differences related to colony handling procedures and analytical platform specified below (instrumentation, software versions, and reference libraries). Colonies were picked from PCA plates for MALDI-TOF MS identification as follows: After determining the TVC, up to three consecutive colonies were selected from a randomly chosen position within a defined countable sector of each PCA plate from day 0/1 and the use-by date for each product, under both storage conditions. Colony material was transferred to the MALDI target plate using a sterile wooden toothpick/application stick. A small amount of biomass was picked from the colony and smeared directly onto the target spot as a thin film. Subsequently, 1 μL of HCCA matrix solution (10 mg/mL α-cyano-4-hydroxycinnamic acid in 50% acetonitrile and 2.5% trifluoroacetic acid) was added to each spot, using a new pipette tip for each position to prevent cross contamination.

In Portugal, spectra were acquired using a MALDI-TOF Biotyper Sirius mass spectrometer (Bruker Daltonics, Germany) and analysed using MBT Compass HT software (version 5.1.450.98) with the MBT Compass HT reference library (version 2023) and FlexControl 3.4 software (Bruker Daltonics). In Norway, spectra were acquired using a Biotyper MALDI-TOF mass spectrometer (Bruker Daltonics, Germany) and processed using MBT Compass 4.1, FlexControl 3.4, and BioTyper 3.1 software, in combination with the MBT 9607 MSP Library (released November 2020) and an in-house reference library. In both cases, spectra were acquired according to the manufacturer's standard measurement procedures.

Instrument calibration was carried out using the Bacterial Test Standard (Bruker Daltonics). Identification scores ≥2.0 were considered reliable for species level identification, while scores between 1.7 and 2.0 were accepted for genus level identification. Scores below 1.7, in the absence of Sanger sequencing confirmation, were considered unreliable and recorded as "NoID".

MALDI-TOF MS was used as complementary culture-dependent evidence to indicate which cultivated taxa were compatible with dominant higher-level 16S rRNA gene amplicon (MiSeq) results, particularly where the amplicon data did not resolve taxa to species level. In addition to MALDI-TOF, BLAST searches of representative sequences from the 16S rRNA gene amplicon sequencing analysis were used to provide additional support for tentative taxonomic interpretation.

2.6. DNA extraction and 16S rRNA gene amplicon sequencing

For DNA analysis, 2–10 mL homogenate per sample were collected immediately after hand-massaging and pelleted by centrifugation at 13,000*g* for 5 min. The pellet was washed in 0.5 mL 1 × PBS, centrifuged again at 13,000*g* for 5 min, and stored at −20 °C until analysis. DNA extraction from pellets was performed with the DNeasy PowerLyser PowerSoil kit (Qiagen, UK) as previously described (Moen et al., 2026).

16S rRNA gene PCR (V4 region) and paired-end sequencing (2 × 150 bp) using MiSeq reagent v3 kits on a MiSeq instrument (Illumina) were performed following the EMP 16S Illumina Amplicon Protocol v.2 with modifications (Caporaso et al., 2023) and protocol by Caporaso et al. (Caporaso et al., 2012) as previously described (Møretrø et al., 2021). Six MiSeq runs were performed, and the resulting demultiplexed raw reads have been deposited in the NCBI archives under BioProject accession no. PRJNA1310835. BioSample IDs for each sample are reported in Supplementary Table 1.

2.7. Microbial diversity analysis

The sequences were processed in QIIME 2 (qiime2-2023.5) (Bolyen et al., 2019). Briefly, the data processing was: demultiplexed using demux, paired ends were joined using vsearch, quality filtered based on a *q*-score above 30, denoised using deblur 16S to generate sub-operational taxonomic units (sOTUs). Taxonomy was assigned using classify-sklearn with the SILVA 99% reference database trimmed to the 515F/806R region (Amir et al., 2017; Bokulich et al., 2013; Bolyen et al., 2019; Hamady and Knight, 2009; Hamady et al., 2008; McDonald et al., 2012; Rognes et al., 2016). Mitochondrial and chloroplast sequences were filtered out. The sOTU level taxonomy table was exported to text files and further processed as described below. A selection of representative sequences was queried against the NCBI BLAST nucleotide database (BLASTN 2.17.0) to obtain additional information about possible species (accessed 04.05.2026).

Counts exported from QIIME 2 were merged and further processed in Python. In total, 720 samples were analysed and, altogether, 3,104 sOTUs were detected from a total of 24,420,901 sequences after removing singletons. The mean number of sequences obtained per sample was 33,918 (max 237,735 and min 1,882). The mean number of sequences per sOTU was 7,868 (max 8,236,081 and min 2).

Alpha diversity was assessed using the Shannon, Simpson and Chao1 indices, as well as observed richness (S_{obs}), calculated using the scikit-bio Python package (v0.7.0). Beta diversity was calculated from counts transformed to relative abundances. For beta diversity analyses on data subsets, only bacteria present in >95% of samples and with a maximum abundance >1% were retained. Filtered taxa were aggregated into a variable named "other" to maintain row sums of 100%. Average abundances were transformed by centered log ratio (CLR) prior to statistical analysis to account for the compositional nature of the data (Gloor et al., 2017). Prior to the CLR transform, zero values were replaced by 0.65 times the lowest value in the data set, as suggested by Lubbe et al. (Lubbe et al., 2021), and the "other" column was adjusted accordingly to keep the row sum constant.

2.8. Bacterial growth modelling

For each production batch and storage scenario, the modified Gompertz model (1) was fitted to the data (Zwietering et al., 1990). Zwietering parameterisation was used as it yields directly interpretable parameters (lag time, maximum growth rate, and asymptotic/maximum population levels). The model is given by:

$$y(t) = y_0 + (y_{max} - y_0) * exp\left\{ - exp\left[\frac{\mu_{max} e}{(y_{max} - y_0)} (\lambda - t) + 1 \right] \right\} \quad (1)$$

where $y(t)$ is the population level at time t ($\log_{10}$ CFU/g), y_0 is the initial value, y_{max} is the upper asymptote, which represents the maximum population, λ is the lag time, μ_{max} is the maximum specific growth-rate parameter and e is Euler's number. Parameters y_0, y_{max}, λ and μ_{max} were estimated by fitting aerobic TVC data ($\log_{10}$ CFU/g) for each individual combination of production batch and storage scenario, using bounded nonlinear least squares with the Trust Region Reflective algorithm (curve_fit, SciPy, v1.16.1). Because the data were sparse, initial parameter values for μ_{max} and λ were first estimated from pooled data within each producer and storage scenario and then used as starting values for batch-specific fits. For the batch-specific models, y_0 was initialised from the mean TVC at the first sampling time, and y_{max}, from the maximum observed TVC, capped at 9 $\log_{10}$ CFU/g. Bounds were set to 0.001–9 $\log_{10}$ CFU/g for y_{max}, pooled estimate ±3 SE for μ_{max}, 0 to the last sampling day for λ, and the initial value ±0.01 $\log_{10}$ CFU/g for y_0. Fits were performed only for batch × scenario combinations with at least four unique sampling time points and maximum observed TVC >3 $\log_{10}$ CFU/g. Approximate standard errors for fitted Gompertz parameters were derived from the covariance matrix returned by curve_fit. Approximate 95% intervals for the parameter estimates were calculated as estimate ±1.96 × SE and should be interpreted as approximate indicators of parameter uncertainty. RMSE and R^2 are reported as descriptive measures of goodness of fit. Parameter estimates, approximate standard errors, approximate 95% intervals, RMSE and R^2 for each batch × storage-scenario fit are provided in Supplementary Table 8. To operationalise shelf life, the fitted Gompertz models were used to estimate the time required for TVC to reach 7 $\log_{10}$ CFU/g (Höll et al., 2016;

Zhang et al., 2012); this predicted time was used as an estimate of shelf life for each batch × storage scenario combination. Because time to 7 $\log_{10}$ CFU/g was derived from the same fitted growth model as λ, associations between these variables were interpreted descriptively rather than as independent validation of a biological mechanism. The limited sampling during the early phase of storage further means that λ estimates should be interpreted as model-derived descriptors of the fitted growth curves rather than as precisely validated measurements of lag duration.

2.9. Sensory evaluation of chicken fillets

Samples from all timepoints described above were included in the sensory analysis. Sensory evaluations were conducted using different panel configurations across the study. For fillets from Producer A, samples from production day 1 were evaluated in two sessions (early and late) by a semi-trained panel (9 members), whereas all subsequent sessions were evaluated by a trained professional panel (10 members). Trained professional assessors undergo regular training and performance monitoring in accordance with ISO 8586:2012, and sensory testing was carried out in facilities compliant with ISO 8589:2007. Samples from Producer B were evaluated by an in-house semi-trained panel trained for this purpose (15 members). Assessors selected for the semi-trained panels (Norway and Portugal) were required to successfully complete a basic taste screening prior to participation. Following selection, the semi-trained panels received structured training in the Attribute Intensity Measurement method (AIM) applied in the study. The AIM method builds upon Quantitative Descriptive Analysis (QDA) according to ISO 13299:2016 General Guidance for establishing a sensory profile and employs the same 15 cm unstructured line scale where intensities are assessed from 1 (no intensity) to 9 (high intensity) for each attribute. In the AIM-method, a smaller number of attributes are assessed than in a traditional QDA (Lawless and Heymann, 2010). Training comprised instruction and practice in the use of intensity scales, with particular emphasis on consistent application of the 1–9 scale. Assessors were further trained in odour recognition and descriptive terminology, including targeted training in identifying odour attributes relevant to raw chicken. In addition, assessors received instruction in standard procedures and appropriate conduct for participation as assessors in sensory analysis.

Fillets to be used in sensory analysis were vacuum packed (<99.0%) and stored in the dark at −40 °C (Producer A) or −20 °C (Producer B). Before evaluation, frozen fillets were thawed overnight at 4 °C. On the day of evaluation, all samples were removed from cold storage 2.5 h prior to serving. Fillets were cut and prepared 30 min before serving. Chicken fillets were prepared according to a standardized procedure applied throughout the study. The ends of each fillet were removed, and the remaining portion was cut transversely into three equal pieces. Each piece was then split longitudinally, resulting in six pieces per fillet. Fillet pieces were placed in white plastic cups and covered with stainless-steel lids.

Panel calibration was conducted prior to the main study through a pre-test. During this calibration phase, samples were evaluated under red light to mask visual differences. Samples were served in a fixed sequence without validation testing. Following individual assessments, the assessors participated in a joint review session in the discussion room, where the stainless-steel lids were replaced with lids labelled BEST–MID–WORST to enable an informed comparative discussion. This calibration procedure was used to align understanding of attributes, intensity scaling, and use of reference points across assessors.

Assessors were provided with a fork and instructed to lift each chicken piece and evaluate odour both from the underside of the fillet and from the headspace within the cup. Samples were evaluated at room temperature and labelled with random three-digit codes. Each assessor was served one piece of fillet (width 2–3 cm, length 3–4 cm, thickness 1–2 cm) per sample.

Odour was evaluated using AIM-method on a 15 cm unstructured line scale from 1 to 9 as described above. Attribute selection was based on prior knowledge of storage related changes in poultry products, preliminary screening of representative samples, and panel consensus discussions to ensure relevance. Eleven odour attributes were included: total intensity, sour/fermented, sweet, cloying, yeasty, ammonia/burning/pungent, sulphur, process, burnt, metallic, and rancid.

Because sensory profiling provides quantitative measurements within a session but only semi-quantitative comparability between sessions (Lawless and Heymann, 2010), absolute intensity scores were not considered directly comparable across sessions. This limitation was particularly relevant for fillets from Producer A, for which two different panels were used. Sensory data were therefore interpreted primarily as within-session and within-producer patterns over storage time and temperature, rather than as directly comparable absolute scores across all sessions.

2.10. Statistical analyses

All statistical analyses were performed separately for fillets from each producer, as they differed markedly in initial microbiota, dominant spoilage organisms, and expected shelf life.

For microbial data, the differences between experimental factors such as storage scenario (temperature) and production days, were assessed using multifactorial analysis of variance (ANOVA). Univariate responses ($\log_{10}$ CFU/g and Gompertz growth parameters) were analysed using univariate ANOVA, while multivariate differences in alpha- and beta diversity were assessed using ANOVA-Simultaneous Component Analysis (ASCA) (Jansen et al., 2005; Khomich et al., 2021). Effect sizes are reported as explained variance (%).

Pairwise correlations among the estimated growth parameters were calculated separately for each producer and storage scenario, using the parameter estimates obtained from Gompertz model fits to each individual batch × storage-scenario combination. Correlation coefficients were calculated in MATLAB using the corr function with default settings, corresponding to Pearson correlation coefficients, and visualized as heatmaps. In contrast, comparisons of pooled batch means for growth parameters were obtained from additive ANOVA models including storage scenario and batch as fixed factors. For these models, pooled batch estimates were compared using the Tukey-Kramer honestly significant difference procedure (multcompare in MATLAB). Because each batch contributed one estimate at 4 °C and one at 8 °C, the pooled batch point estimates are equivalent to the arithmetic mean of the two scenario-specific estimates, whereas the comparison intervals depend on the ANOVA residual variance and the Tukey-Kramer adjustment.

Sensory data were analysed at the session level. Principal component analysis (PCA) was performed separately for each sensory session to assess the dimensionality of sensory change during storage. Attribute intensities were also ranked descriptively within each session. LOESS regression (R function loess with span 1) was used to visualise total intensity as a function of storage day and, separately, as a function of TVC. To evaluate the relationship between sensory changes and microbiology, Pearson and Spearman rank correlations were calculated between sensory attributes and bacterial load ($\log_{10}$ CFU/g), both overall and by sensory session.

3. Results

3.1. Initial microbial load and composition of fresh chicken

Analyses of fresh chicken breast fillets on the day of slaughter (day 0; Producer B) or the day after slaughter (day 1; Producer A) were performed to determine the initial TVC and to characterise the initial bacterial community composition. Statistical analyses then examined variation between production days and sampling times within the same day.

Mean initial TVC were lower at Producer A (2.4 $\log_{10}$ CFU/g; range 1.3–3.0) than at Producer B (4.3 $\log_{10}$ CFU/g; range 3.3–5.4) (Fig. 1).

Both producers showed an approximately 2-log difference between the batches with the lowest and highest TVC. For both producers, initial TVC tended to be higher during the warmer months. For Producer A, the highest initial loads were observed in batches A2 to A4, corresponding to production in May and August (Table 2). For Producer B, initial TVC increased progressively from batches B1 to B5, spanning production from February to July (Table 2).

The microbiota of fresh chicken breast fillets was noticeably different between the two producers, with a higher abundance of *Bacillaceae* and *Lactobacillus* spp. in fillets from Producer A, and *Pseudomonas* spp., *Yersiniaceae* and *Brochothrix* spp. in fillets from Producer B (Fig. 2).

Overall, the ten most prevalent bacterial taxa in fresh chicken fillets (mean relative abundance across both producers) were, at mixed taxonomic rank (families and genera): *Bacillaceae* (14.7%), *Pseudomonas* (12.6%), *Lactobacillus* (12.2%), *Yersiniaceae* (8.8%), *Acinetobacter* (6.3%), *Brochothrix* (2.8%), *Chryseobacterium* (1.9%), *Faecalibacterium* (1.9%), *Bacteroides* (1.8%), and *Psychrobacter* (1.7%).

Between-day differences were the major source of variation in both TVC and microbiota in fresh chicken fillets. For Producer A, production day explained 39% of the variance in TVC, 48% in alpha diversity and 47% in beta diversity (all $p < 0.001$), exceeding the main effect of time of day (early vs. late: 16%, 9%, and 10%, respectively). The day × time interaction was also substantial (21%, 17%, 19%; $p \leq 0.004$), indicating that early-late differences depend on production day. For Producer B, the dominance of production day was even stronger, explaining 86% of TVC and 58% and 54% of alpha- and beta diversity, respectively (all $p < 0.001$), whereas the main effect of time of day was small (TVC 2%, $p = 0.032$; α 6%, $p = 0.002$; β 9%, $p < 0.001$). The interaction was negligible for TVC (3%, $p = 0.26$) but remained evident for the microbiota (21% for α and 17% for β; both $p < 0.001$) (Supplementary Tables 2 and 3). Consistent with these results, the ASCA score plots indicated day-to-day structuring in both datasets. Clustering by production day was strong for Producer B, whereas several production days overlapped for Producer A, indicating more moderate between-day separation. Early-late shifts within a production day were present in both datasets but were more pronounced for Producer A (Supplementary Figs. 1, 2, and 3). Loadings indicated that separation along PC1 reflected overall alpha diversity, with all metrics loading positively.

For Producer A, several late batches (A1, A2, A4, and A5) were characterized by higher relative abundances of *Bacillaceae* and were accompanied by lower alpha diversity than the corresponding early batches (Supplementary Figs. 1 and 2). Production day A6 showed high *Bacillaceae* abundance and low alpha diversity in both early and late samples and was the only production day where the late batch had a higher TVC than the early batch. In contrast, production day A3 showed low *Bacillaceae* abundance and high alpha diversity in both early and late samples (Supplementary Figs. 1 and 2).

For Producer B, consistent with the stronger production day effect, individual days showed distinct microbial profiles: production day B1 combined lower TVC with high relative abundances of *Pseudomonas* and *Brochothrix*; the late batch from B1 also exhibited higher alpha diversity than the other batches (Fig. 1, Fig. 2, Supplementary Figs. 1 and 3). Production day B2 was marked by higher abundances of *Lactobacillus*, whereas production day B5 stood out with a markedly elevated initial TVC relative to all other production days (Fig. 1B), together with low alpha diversity, and an increased relative abundance of *Yersiniaceae* (Fig. 2, Supplementary Figs. 1 and 2).

Overall, fresh chicken fillets showed clear differences between the two producers in both initial TVC and microbiota composition, with production day emerging as the dominant source of variability within each producer.

3.2. Microbial growth dynamics during storage

Storage experiments were conducted under two temperature scenarios: stable storage at 4 °C and a temperature shift from 4 °C to 8 °C (see Materials and methods). At predefined time points, TVC was quantified and microbiota composition (alpha- and beta diversity) were characterized to capture temporal changes during storage. The products from the two producers appeared to differ markedly in bacterial growth dynamics during storage (Fig. 3 and Fig. 4).

Maximum specific growth rates (μ_{max}) were comparable between producers, whereas products from Producer B tended to exhibit shorter lag times (λ) and a higher estimated upper asymptote (y_{max}) than those from Producer A. As expected, μ_{max}-values were higher under the temperature-shift scenario for both producers. In contrast, lag times did not differ significantly between storage scenarios (Supplementary Tables 4 and 5), consistent with the shared initial 4 °C storage period in both scenarios.

Accordingly, the predicted time required to reach 7 $\log_{10}$ CFU/g differed significantly between storage scenarios and was consistently longer for Producer A than for Producer B (Fig. 5, Supplementary Tables 4 and 5). For Producer A, this time ranged from 16 to 29 days at stable 4 °C (mean 21 days), and from 12 to 20 days under temperature shift to 8 °C (mean 14 days). For Producer B, the corresponding times were 8 to 17 days at stable 4 °C (mean 11 days) and 6 to 10 days under

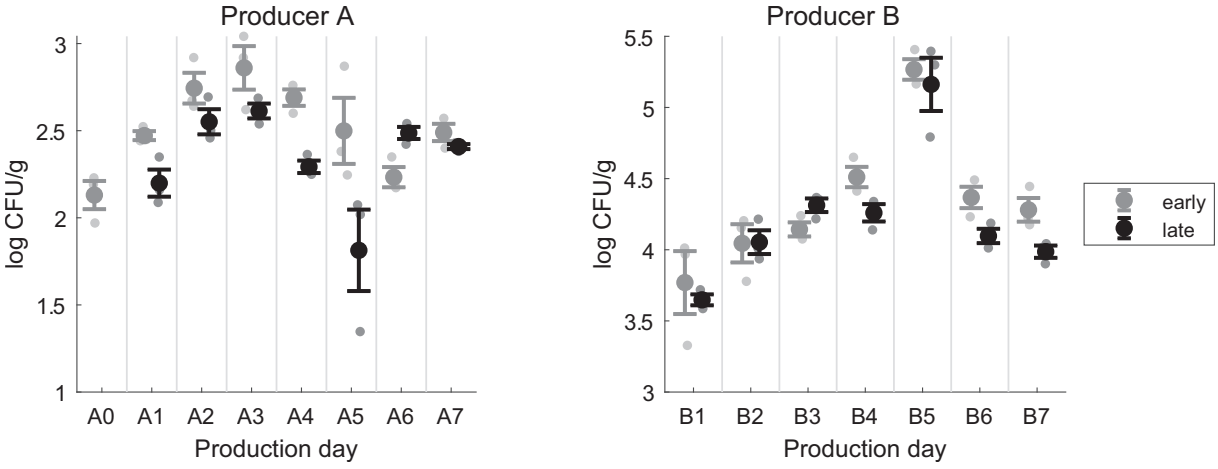

Fig. 1. Total viable counts (TVC; $\log_{10}$ CFU/g) in MAP-packaged chicken fillets for each production day, shown separately for Producer A (left) and Producer B (right). Small points represent individual packages (raw measurements, jittered), and large points show batch means (early = grey; late = black). Error bars indicate mean ± SEM within batch. Early and late batches are shown side-by-side for each production day.

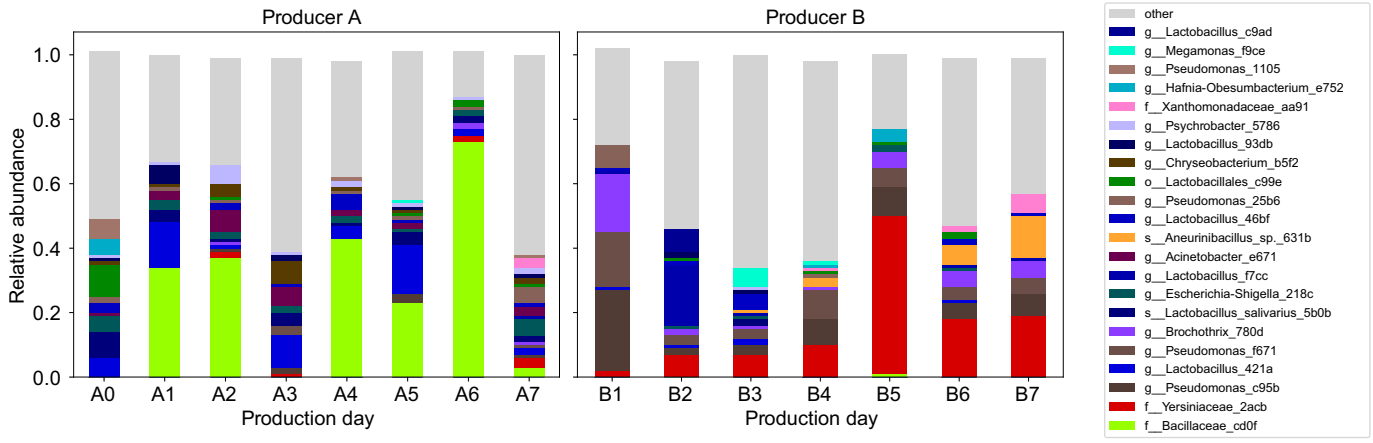

Fig. 2. Dominant microbiota in fresh chicken breast fillets. Stacked bar plots show the relative abundance of dominant bacterial taxa across production days for producers A and B. For each production day, early and late batches were combined (i.e., batch timing is not shown separately in this figure). Taxa belonging to the same genus are represented using different shades within the same colour palette (e.g., all *Lactobacillus* spp. sOTUs are shown in varying tones of blue). Colours are kept consistent across microbiota figures for shared taxa to facilitate comparison between fresh and late-shelf-life communities. The category "other" comprises taxa below the dominance threshold.

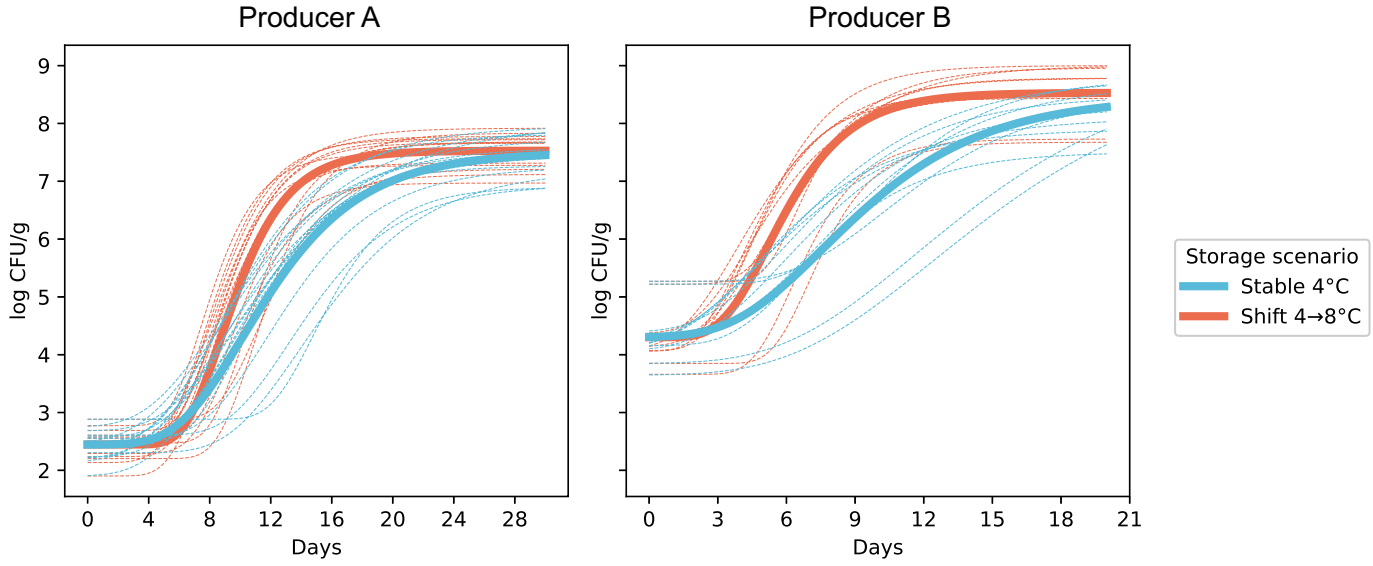

Fig. 3. Bacterial growth during storage. Estimated average growth curves for each producer and storage scenario are given in bold; blue = stable 4 °C; red = shift from 4 to 8 °C. Dashed lines represent growth curves fitted to individual production batches. Estimated TVC growth curves for all batches are given in Supplementary Fig. 4.

temperature shift to 8 °C (mean 7 days).

Variation in time to reach 7 $\log_{10}$ CFU/g was driven by both storage scenario and production batch (Supplementary Tables 4 and 5). Because missing data resulted in an unbalanced design, production day and time of day were not analysed separately for the storage data but were combined into the single factor batch. For Producer A, storage scenario explained 43% of the variance and batch explained 53%. For Producer B, the corresponding effects were 49% for scenario and 44% for batch (Supplementary Tables 4 and 5). Visually, these batch differences appeared to align more strongly with production day than with early-late differences within the same production day (Fig. 5).

Across producers and storage scenarios, time to reach 7 $\log_{10}$ CFU/g increased with lag time (r = 0.69–0.88), indicating that longer lag phases were associated with longer times to reach this threshold (Supplementary Fig. 7). This association should be interpreted with caution, because both λ and time to 7 $\log_{10}$ CFU/g originate from the same Gompertz fit and are therefore not statistically independent. By contrast, the fitted initial TVC (y_0) showed little association with time to 7 $\log_{10}$ CFU/g overall and was slightly negative for fillets from Producer B (r = −0.31 and −0.24), indicating that initial counts mattered less than subsequent growth dynamics in the fitted models. The association with the upper asymptote (y_{max}) varied by producer and scenario: it was negative for Producer A in both scenarios (r = −0.86 and − 0.76) and for Producer B under temperature shift (r = −0.78), but moderately positive for Producer B at stable 4 °C (r = 0.44) (Supplementary Fig. 7).

For Producer A, time to 7 $\log_{10}$ CFU/g showed only weak correlations with day 1 aerobic TVC (r = 0.18 and 0.16), similar to those observed for the fitted initial levels (y_0). Initial counts measured under product-like MAP conditions showed a stronger association with time to 7 $\log_{10}$ CFU/g than the corresponding aerobic counts (r = −0.38 and −0.55) (Supplementary Fig. 7). These observations are consistent with the interpretation that methodological alignment between enumeration conditions and the actual package environment can influence the predictive value of initial counts (Moen et al., 2026). For Producer B, product-like MAP counts were available only for the first production round (B1) and are reported in Supplementary Table 1; these data were

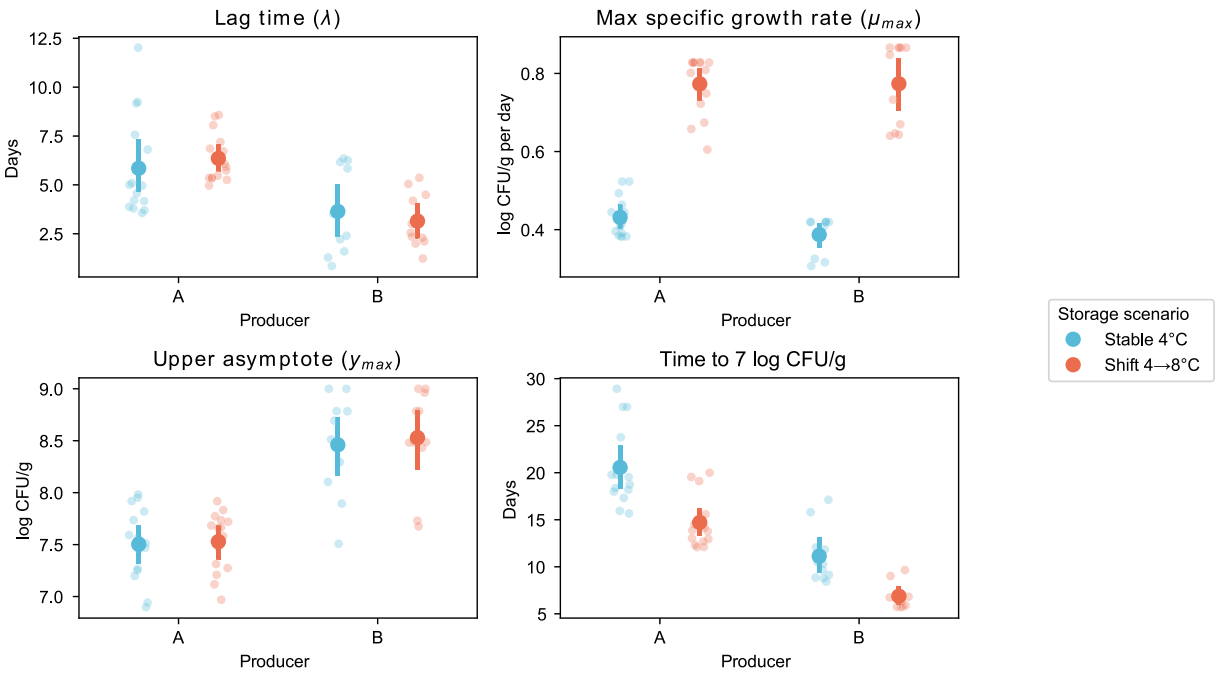

Fig. 4. Estimated growth parameters obtained from Gompertz model fitting. Bold dots and lines indicate the means and corresponding 95% confidence intervals. Opaque dots represent parameter estimates for individual batches.

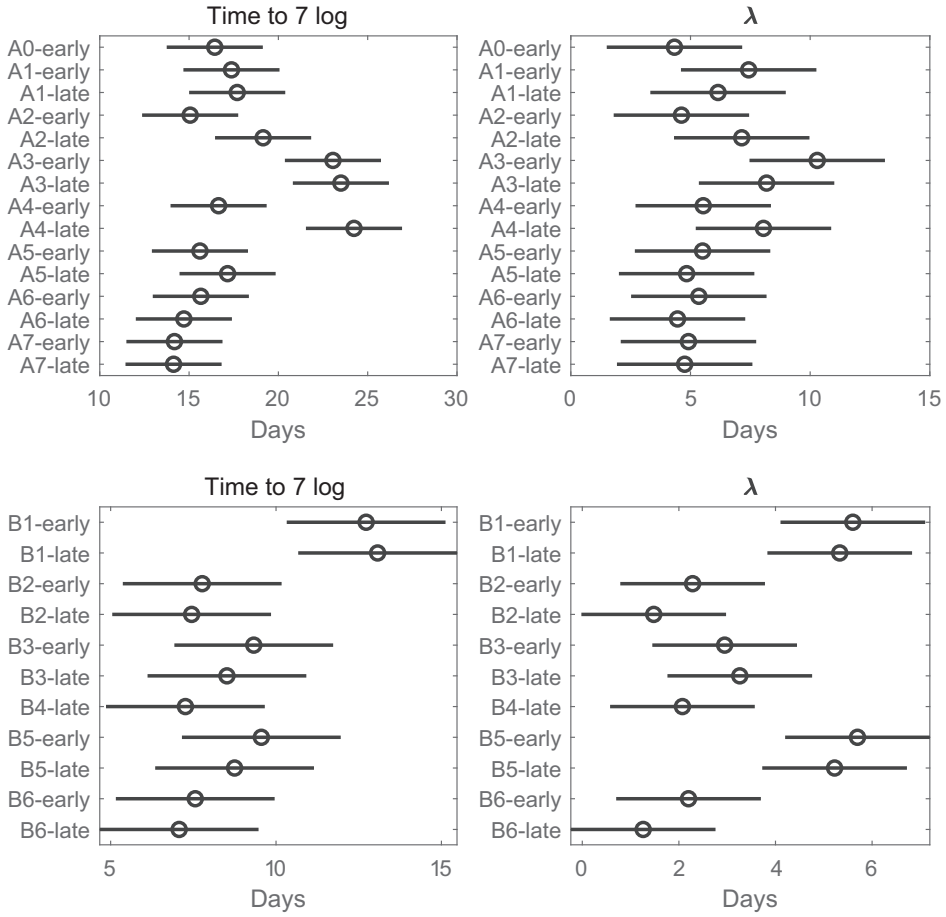

Fig. 5. Multiple comparisons of batch means for time to reach 7 $\log_{10}$ CFU/g (Time to 7 log) and lag time (λ) for Producer A (top row) and Producer B (bottom row). The 95% comparison intervals (horizontal lines) were calculated using the Tukey-Kramer honestly significant difference (HSD) method; thus, non-overlapping intervals indicate statistically significant differences between batch means. Estimates are pooled across storage scenarios (stable 4 °C and 4 to 8 °C temperature shift). Results for the remaining Gompertz parameters are provided in Supplementary Figs. 5 and 6.

therefore not included in the across-production-day correlation analyses. Associations between time to 7 $\log_{10}$ CFU/g and TVC measured later in storage were stronger and inverse: for Producer A, TVC at day 7 was strongly inversely correlated with time to 7 $\log_{10}$ CFU/g ($r = -0.91$ and -0.87), whereas for Producer B the corresponding correlations were moderate under stable storage at day 5 ($r = -0.59$ and -0.56) and stronger under temperature shift at day 4 ($r = -0.84$ and -0.81) (Supplementary Fig. 7). These inverse correlations were expected to be stronger for later TVC measurements, because these samples were taken closer to the end of lag phase or after the onset of faster growth, when differences in remaining time before the 7 $\log_{10}$ CFU/g threshold become more directly reflected in the observed counts.

Together, these results indicate that variation in the model-derived time to 7 $\log_{10}$ CFU/g was most strongly associated with the model-derived lag time, although this relationship is partly structural because both parameters were derived from the same fitted growth model. In contrast, initial TVC (fitted or aerobic) showed little association, and relationship with upper asymptote was inconsistent across producers and storage scenarios.

3.3. Microbiota at late shelf life

To identify the bacterial groups dominating near the end of shelf life, the microbiota of samples with TVC ≥ 7 $\log_{10}$ CFU/g was analysed. This threshold was used as an operational comparative benchmark, rather than as a universal sensory rejection threshold, to enable comparison of communities at a similar late-stage microbiological level across batches and storage scenarios.

Although the initial microbiota of fresh chicken fillets from both producers was highly diverse, storage led to the emergence of distinct communities associated with each producer and dominated by only a few bacterial groups. At this stage, microbiota composition grouped primarily by producer, with no systematic separation between early and late batches (Supplementary Figs. 8 and 9). Samples were therefore pooled across time of day for presentation in Fig. 6.

Stored chicken fillets from Producer A were dominated by *Lactobacillales* and *Hafnia-Obesumbacterium*, while fillets from Producer B showed high abundances of *Brochothrix* and *Yersiniaceae* (Fig. 6). The sOTUs identified as *Lactobacillales* and *Yersiniaceae* can encompass a wide range of genera. Complementary MALDI-TOF MS and BLAST searches of representative sequences were consistent with the presence of isolates identified as *C. divergens* and *S. proteamaculans*, respectively, but species-level assignment of the corresponding amplicon taxa should be regarded as tentative. Similarly, the sOTUs assigned to *Hafnia-Obesumbacterium* and *Brochothrix* were consistent with the presence of isolates identified as *H. alvei* and *B. thermosphacta*.

Under stable storage at 4 °C, CO_2-tolerant Gram-positive spoilage-associated taxa dominated the microbiota, with *Lactobacillales* dominating fillets from Producer A and *Brochothrix* dominating fillets from Producer B (Fig. 6). In both cases, the temperature shift from 4 °C to 8 °C was associated with increased relative abundances of *Enterobacterales*, namely *Hafnia-Obesumbacterium* for Producer A and *Yersiniaceae* for Producer B. However, the magnitude of this shift differed between producers: microbiota composition in fillets from Producer A was more strongly affected, consistent with storage scenario explaining a larger proportion of the beta diversity variation than in Producer B (16% vs. 5%; Supplementary Tables 4 and 5). This producer difference co-occurred with lower initial TVC in Producer A.

As shown in Fig. 6, the late-shelf-life microbiota was largely consistent across production days within each producer, with no systematic day-to-day shifts in dominant taxa. Minor deviations were observed for individual production days, but these did not alter the overall community structure associated with each producer. These patterns were consistent with multivariate analyses (ASCA) presented in Supplementary Figs. 8 and 9, confirming the overall producer associated community structure at late shelf life.

3.4. Sensory development during storage

Sensory data were analysed to describe changes in odour intensity

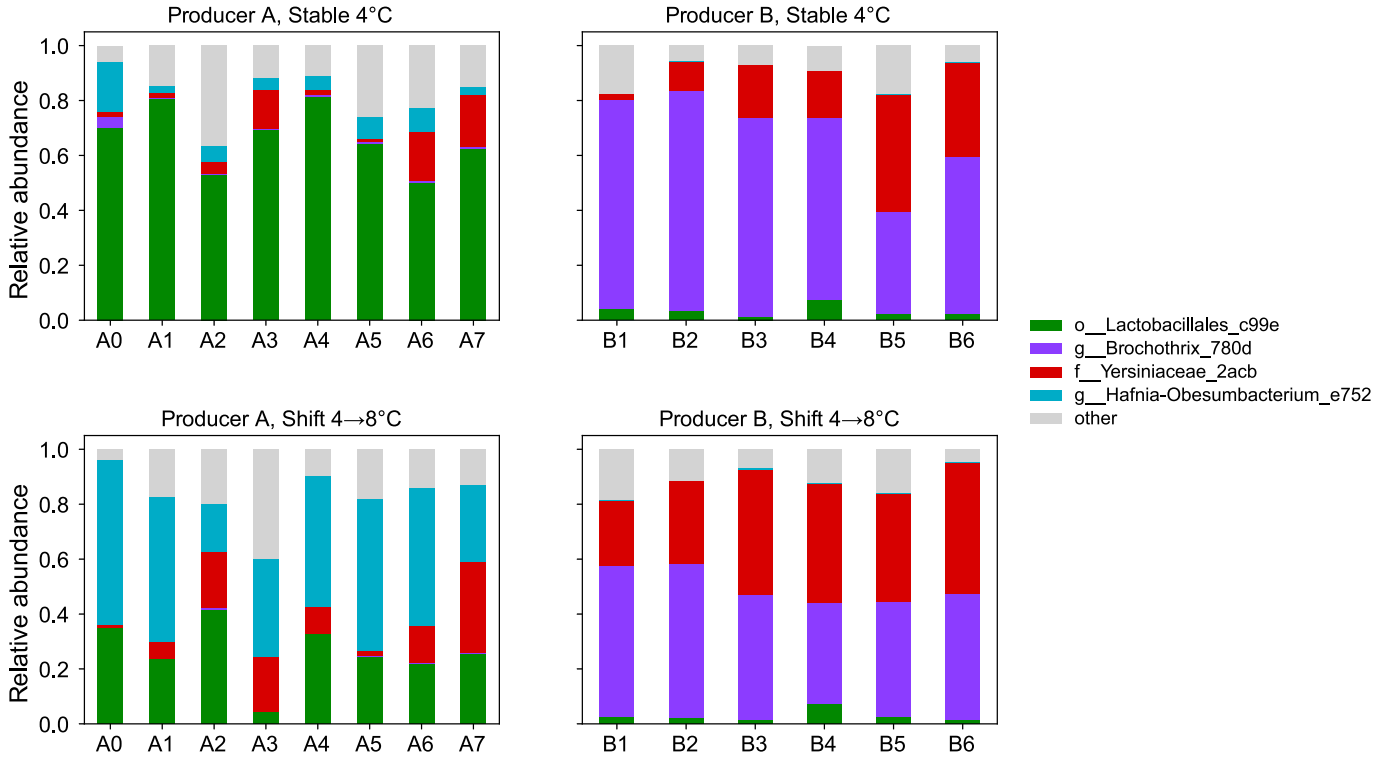

Fig. 6. Relative abundances of dominant bacterial taxa in chicken fillets at late shelf life from Producers A and B under the two storage scenarios. Only samples with $\log_{10}$ CFU/g > 7 were included. Values represent mean relative abundances across samples within each producer, storage scenario, and production day.

and key descriptive attributes during storage under the two temperature scenarios and to assess whether these changes tracked microbial growth within each producer. Because samples were assessed by different panels/sessions (Materials and methods), comparisons focus on within-session and within-producer patterns over time and temperature rather than absolute intensity levels across sessions or producers. Details of the sensory sessions, panels, and evaluated odour attributes are provided in Supplementary Tables 6 and 7.

PCA showed that sensory changes during storage were effectively one-dimensional, with PC1 explaining 80–97% of the variance across sessions for Producer A and >95% for Producer B (Supplementary Figs. 10 and 11). This indicates that, within each producer, storage changed the sensory profile in broadly the same way at both temperatures. Higher temperature mainly accelerated this development, rather than producing a different pattern of odour attributes. All odour attributes increased during storage, and for fillets from both producers, total intensity, cloying, and sour-fermented were among the three most intense attributes. The strong correlation among all attributes suggested that total intensity captured most of the sensory variation and provided a practical metric for linking sensory and microbial development. This pattern was observed despite clear differences in the dominant late-shelf-life microbiota between fillets from the two producers.

LOESS regression showed that total intensity increased with storage time, and that higher temperature accelerated this development (Fig. 7). The relationship with bacterial load was then examined by correlation analysis of sensory attributes against TVC (Table 3, and Supplementary Tables 6 and 7). Across all sensory sessions, the Spearman correlations between total intensity and TVC were $\rho = 0.69$ for fillets from Producer A and $\rho = 0.71$ for fillets from Producer B. Among the individual odour attributes, the highest Spearman correlation was observed for sour-fermented for fillets from Producer A and for ammonia/burning/pungent for fillets from Producer B ($\rho = 0.75$ and 0.74, respectively) (Table 3). When examined within individual sensory sessions, correlations between total intensity and TVC varied but remained consistently moderate to high, ranging between $\rho = 0.57$–0.96 for fillets from Producer A and $\rho = 0.58$–0.93 for Producer B (Supplementary Tables 6 and 7). The relationship with TVC was further visualized using LOESS regression, which showed that total intensity increased with TVC in a similar pattern at both temperatures, with higher temperature mainly accelerating progression rather than altering the overall pattern (Fig. 8).

Overall, the sensory results supported the microbial data by showing that odour changes, with total intensity as a practical summary attribute, closely tracked TVC within each producer across sensory sessions and storage scenarios.

Table 3
Pearson and Spearman correlations between each sensory attribute and mean observed TVC ($\log_{10}$ CFU/g) overall.

Sensory attribute	Producer A		Producer B	
	Pearson	Spearman	Pearson	Spearman
Total intensity	0.61	0.69	0.73	0.71
Ammonia/burning/pungent	0.53	0.58	0.72	0.74
Burnt	0.24	0.38	0.38	0.42
Cloying	0.50	0.57	0.71	0.73
Metal	0.12	0.11	0.64	0.64
Process	0.17	0.23	0.24	0.24
Rancid	0.14	0.04	0.38	0.38
Sour fermented	0.73	0.75	0.69	0.71
Sulphur	0.42	0.60	0.31	0.44
Sweet	0.24	0.12	0.56	0.58
Yeasty	0.37	0.31	0.63	0.68

4. Discussion

Adaptive, data-driven shelf-life determination requires systematic, predictable variation so that microbiological measurements taken at production or early during storage can support robust labelling decisions. In this context, the present results showed that variation over production days was the clearest and most useful source of structured variation within each producer, whereas differences between early and late batches sampled on the same production day were smaller and less consistent. Accordingly, the data supported the hypothesis that microbial shelf-life variation was systematically structured by production day, while providing only partial support for consistent early-late batch differences within the same production day. The stronger production-day structure likely reflects the combined influence of factors that vary from one day to the next, such as weather conditions and changes in the processing plant environment (e.g., cleaning efficacy or pre-production drying) (Rouger et al., 2017; Sequino et al., 2025). Early–late batch differences were smaller, not directionally consistent across production days, and were therefore less useful than production day as a grouping factor for adaptive shelf-life decisions. We assessed this within-day

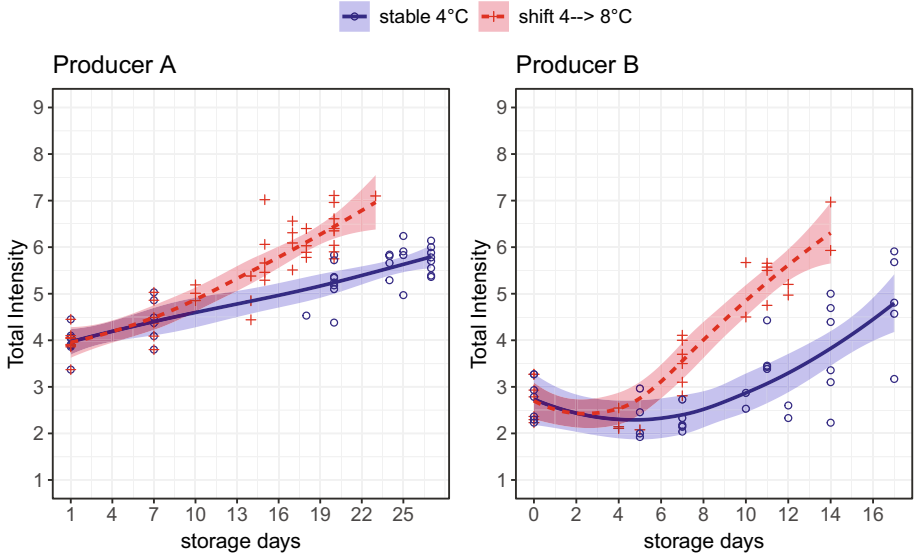

Fig. 7. LOESS regression of total intensity against storage day for stable 4 °C (blue) and temperature shift from 4 °C to 8 °C (red), shown separately for Producer A (left) and Producer B (right). Symbols represent observed total intensity values across production days. Production day 1 for Producer A was excluded because it was evaluated by a different panel using a different part of the scale. Absolute intensity should not be compared directly between producers.

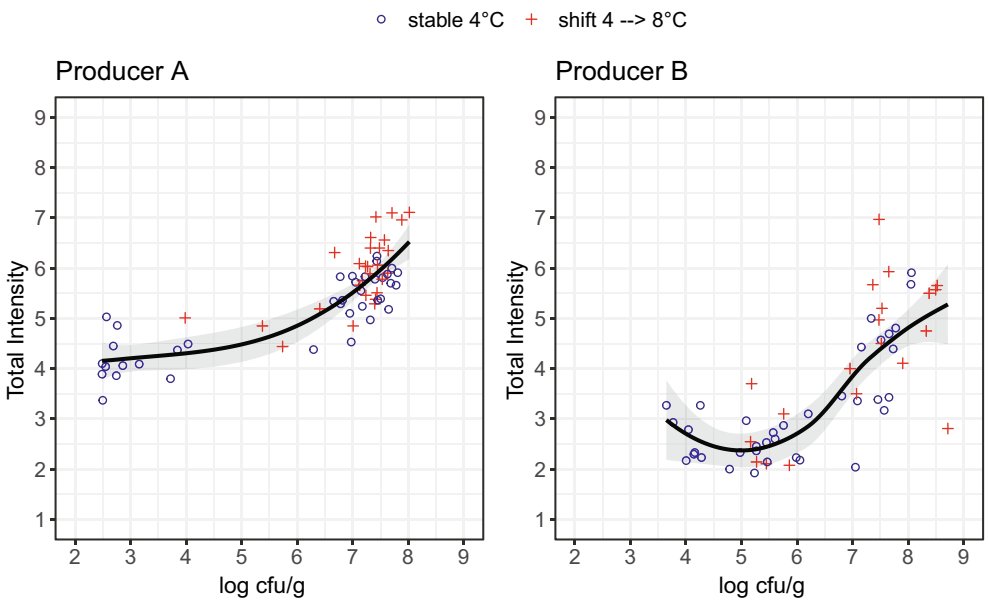

Fig. 8. LOESS regression of total intensity against mean observed TVC (log_{10} CFU/g) for both storage temperatures combined, shown separately for Producer A (left) and Producer B (right). Production day 1 for Producer A is excluded since the panels used scales differently. Absolute intensity should not be compared directly between producers.

hypothesis because time-of-day patterns have been reported in salmon processing, with early versus later fillets differing in spoilage bacteria, and poultry studies document processing-environment reservoirs and cross-contamination that could plausibly generate shift-dependent patterns (Chen et al., 2020; Lauritsen et al., 2019; Møretrø and Langsrud, 2017). In the present study, however, the observed within-day differences were non-systematic and probably reflected a mixture of flock-to-flock variation and shift-specific processing effects rather than a reproducible time-of-day pattern.

By contrast, the hypothesis that higher initial TVC would predict shorter shelf life was not supported when fillets from the two producers were analysed separately. Within each producer, shelf-life variation was more closely linked to the model-derived lag time parameter (λ) than to initial aerobic TVC. Because both λ and time to 7 log_{10} CFU/g were derived from the same Gompertz fit, this association should be interpreted as a model-based description of the fitted growth curves rather than as independent evidence that shelf life was determined by an adaptation phase of the whole bacterial community. Under MAP, initial aerobic TVC is likely to have limited predictive value because it includes both bacteria that are relevant for later spoilage and background bacteria that may be inhibited by the package atmosphere or otherwise fail to dominate during storage (Höll et al., 2016; Kolbeck et al., 2020; Lauritsen et al., 2019; Marmion et al., 2021). The apparent lag in total aerobic TVC may therefore reflect the time required for the spoilage-associated, MAP-selected fraction to increase from low initial abundance until it contributes substantially to total counts. This helps explain why initial aerobic TVC showed little relation to time to 7 log_{10} CFU/g within either producer, even though there were clear differences in both initial counts and shelf life. Thus, although differences in initial TVC coincided with broad shelf-life differences between the two producers, initial aerobic TVC had limited predictive value for explaining batch-to-batch shelf-life variation within each producer under the MAP conditions studied.

This interpretation is supported by several observations and aligns with the specific spoilage organism (SSO) framework emphasised in EFSA guidance, which recommends identifying the relevant spoilage microorganisms and assessing their growth under the intended packaging and storage conditions rather than relying on total counts alone (Hazards et al., 2020). Time to 7 log_{10} CFU/g showed robust associations with later TVC measurements (e.g., day 7 TVC for Producer A), indicating that the useful signal becomes clearer once spoilage-associated bacteria have already gained ground in the product. Consistent with this, for Producer A, correlations with time to 7 log_{10} CFU/g were stronger when initial TVC was measured under product-like MAP conditions rather than aerobically. These observations reinforce that the predictive value of initial counts depends on how well the enumeration conditions capture the bacteria selected by the actual package environment (Moen et al., 2026). They also point to early growth dynamics of spoilage-associated bacteria as more relevant for shelf-life development than initial aerobic TVC alone. However, λ should not be over-interpreted as an early lever for shelf-life setting. In this study, λ was estimated from Gompertz fits rather than measured directly, and its precision was constrained by limited sampling during the first days of storage. Fit diagnostics and approximate parameter uncertainty for the batch-specific Gompertz models are provided in Supplementary Table 8, and the corresponding fitted curves together with observed TVC data are shown in Supplementary Fig. 4. Although the fitted curves generally showed good agreement with the observed TVC trajectories, λ was weakly estimated in some batch × storage-scenario fits, as indicated by standard errors that were large relative to the corresponding estimates. Thus, good trajectory-level fit does not necessarily imply precise estimation of λ. Accordingly, λ should be interpreted as a model-derived descriptor of fitted early growth behaviour rather than as a precisely estimated measure of lag duration. The absence of a significant storage-scenario effect on λ should also be interpreted in relation to the experimental design, where all products were initially stored at 4 °C until day 3 for Producer B or day 7 for Producer A. These periods closely matched the estimated lag times, meaning that the temperature shift occurred largely after the estimated lag phase had elapsed, rather than as evidence that lag duration is generally insensitive to temperature. The practical implication is not that λ itself can presently be used as a release-time decision variable, but that future adaptive shelf-life approaches under MAP may require early follow-up measurements after a few days of storage to better capture the development of spoilage-associated bacteria. Practical shelf-life adjustment at release would require validated indicators available before product distribution. However, follow-up measurements collected after a few days of storage could still provide valuable information for downstream predictive models, once sufficient

storage information has accumulated. Such model outputs could potentially be communicated to downstream actors through digital information systems, for example via QR codes, apps, or other barcode-linked data layers (Li and Wang, 2017). Implementation would require further development and validation of robust indicators and prediction models before operational use.

Although 7 $\log_{10}$ CFU/g does not by itself define sensory rejection, it was used as an operational comparative microbiological benchmark in the present study because it provided a common late-storage reference point across batches and storage scenarios. Within each producer, odour development was correlated with increasing TVC, while higher temperature mainly accelerated sensory change rather than producing a qualitatively different odour pattern. Thus, time to 7 $\log_{10}$ CFU/g functioned as a practical marker of spoilage progression in this dataset, even though it should not be interpreted as a universal sensory cut-off. This interpretation is also consistent with previous poultry studies in which spoilage has been linked to microbial levels around 7 $\log_{10}$ CFU/g in some product-specific settings, while more noticeable odour changes in raw chicken have often been observed at higher counts, typically above 8 $\log_{10}$ CFU/g (Katiyo et al., 2020; Spyrelli et al., 2021). At the same time, recent work on cooked MAP chicken shows that sensory differentiation does not necessarily follow a universal TVC threshold, reinforcing that microbial counts should be interpreted in relation to product type, storage conditions and the mode of sensory evaluation (Söderqvist et al., 2024). Differences in spoilage-associated community composition may further shift the relationship between bacterial counts and sensory rejection (Marmion et al., 2021).

Given potential panel and session effects, sensory results were interpreted in terms of relative development over storage time and temperature within each producer, rather than as absolute differences in intensity across sessions or producers. This limitation was reinforced by the sensory sample handling, as samples were frozen prior to evaluation and stored at different frozen-storage temperatures for the two producers (−40 °C for Producer A and −20 °C for Producer B). Because freeze-thaw handling may affect volatile profiles and odour perception, this may have further limited direct comparability of absolute sensory scores between producers.

The apparent stability of the late-shelf-life microbiota within each producer was one of the clearest ecological findings in this study. Although the microbiota in fresh fillets varied between production days, refrigerated storage under MAP repeatedly selected a limited set of dominant taxa, with *Lactobacillales* and *Hafnia-Obesumbacterium* dominating in fillets from Producer A and *Brochothrix* and *Yersiniaceae* dominating in fillets from Producer B. Similar convergence towards a limited set of dominant spoilage taxa in MAP poultry has been reported previously, although the taxa involved depend on the packaging atmosphere and storage conditions (Höll et al., 2016; Lauritsen et al., 2019). The repeated sampling over one year extends previous MAP poultry studies by showing that this convergence was not limited to individual batches but recurred across production days within products from each producer despite variation in the initial microbiota. This suggests that taxa consistently selected during refrigerated MAP storage may provide useful information for future adaptive shelf-life approaches, potentially complementing day-to-day variation in total counts alone. Such recurrent communities may reflect a combination of product characteristics, MAP conditions, and microbiota repeatedly introduced or selected within each production chain, but the present design does not allow these factors to be separated. Beyond spoilage prediction, microbiota that are repeatedly selected during refrigerated MAP storage may also be relevant for future precision food-safety research. Because poultry is frequently associated with foodborne pathogens and outbreaks, such recurrent communities could influence pathogen prevalence, persistence, resilience or survival. Although the present study did not quantify foodborne pathogens or test pathogen-microbiota interactions, future studies could examine whether recurrent microbiota selected during refrigerated MAP storage influence the prevalence, resilience, or survival of relevant pathogens.

The results are also consistent with the general MAP literature, where elevated CO_2 suppresses aerobic spoilers such as *Pseudomonas* and promotes facultative anaerobes and other CO_2-tolerant bacteria, including lactic acid bacteria and *Brochothrix* (Höll et al., 2016; Jimenez et al., 1997; Lauritsen et al., 2019; Söderqvist et al., 2024). However, because the two producers differed in several linked factors, including production environment, chicken breed, product format, shelf-life regime and MAP composition, the observed differences between products from the two producers should be interpreted descriptively rather than causally. Estimating the independent contribution of MAP composition would require an experimental design with controlled manipulation or standardisation of gas composition.

The temperature shift from 4 °C to 8 °C modified the microbiota development, most notably by increasing *Enterobacterales* (*Hafnia* and *Yersiniaceae*) at late shelf life. This temperature shift-related change in the microbiota was more pronounced in fillets from Producer A than Producer B, consistent with storage scenario accounting for a larger share of beta diversity variation in Producer A. One plausible explanation is that fillets from Producer A had lower TVC when moved to 8 °C, making the microbiota composition more responsive to temperature shift. The combination of higher initial TVC including CO_2-tolerant bacteria may explain why Producer B fillets exhibited shorter lag phases and reached 7 $\log_{10}$ CFU/g sooner than Producer A fillets. The CO_2-containing high-O_2 MAP used by Producer B may have favoured the increase and late shelf-life dominance of *Brochothrix* consistent with previous studies (Sarfraz et al., 2021). However, *Brochothrix* was already present at substantial relative abundance at packing, indicating that atmosphere composition alone is unlikely to explain its dominance.

Interestingly, although fillets from the two producers differed in lag time (λ), upper asymptote (y_{max}), and late shelf-life microbiota, the estimated maximum growth rate (μ_{max}) was similar. This suggests that, within the fitted models, differences in shelf-life development were driven mainly by lag duration and maximum population level rather than by large differences in the estimated exponential growth rate. The similar μ_{max} estimates should therefore be interpreted cautiously and may reflect the shared storage-temperature regime and the fact that both products were raw chicken fillets, rather than indicating that the dominant spoilage taxa had identical growth behaviour. In contrast, differences in the fitted upper asymptote may reflect differences in the maximum population levels supported under the respective product and packaging conditions. More generally, this is consistent with temperature as a dominant external driver of microbial growth kinetics and shelf-life loss in refrigerated foods (Albrecht et al., 2020; Labuza et al., 1997). In practical terms, this makes time-temperature indicators (TTIs) or other temperature-history tools relevant for adaptive, data-driven shelf-life management. At the same time, the present results indicate that temperature alone is unlikely to explain all relevant variation, since fillets produced on different production days still differed in lag time and time to 7 $\log_{10}$ CFU/g. Temperature-history tools may therefore be most useful when combined with producer or production day level adjustment, rather than used as stand-alone package-level solutions. A key next step will be to identify robust, measurable indicators for spoilage-associated taxa or early growth behaviour that can be assessed at production and integrated with temperature-history information for adaptive shelf-life determination. However, practical implementation will also depend on analytical costs, integration with downstream information systems, and whether predictable variation is large enough to support meaningful waste reduction under real consumer-handling conditions. Future validation studies should also be designed to separate MAP effects from broader producer-related factors, for example by manipulating MAP composition within a single producer or by applying a standardized MAP across producers while keeping raw material, product format and storage conditions as comparable as possible. Such controlled designs would clarify whether recurrent spoilage communities and shelf-life variation are driven primarily by

packaging atmosphere, production-environment factors, or their interaction.

5. Conclusions

This study examined whether batch-to-batch variation in the microbiological status and growth dynamics of MAP-packaged chicken breast fillets is sufficiently structured and predictable to inform adaptive, data-driven shelf-life determination. The primary aim was to evaluate whether microbial and shelf-life variation was systematically structured over time within each producer, rather than to identify the specific factors underlying differences between the two producers. Variation was most strongly structured at the production-day level: production day was the most consistent grouping factor for both initial microbial status and shelf-life development, whereas differences between batches produced on the same day were smaller and inconsistent. The results therefore support the hypothesis that production-day effects are systematic and relevant for shelf-life decisions, while providing only limited support for within-day batch effects as a basis for shelf-life adjustment. Initial aerobic TVC did not explain within-producer variation in shelf life. Instead, the time required to reach 7 $\log_{10}$ CFU/g was most strongly associated with the model-derived lag parameter (λ), although this relationship is partly structural because both variables were derived from the same growth model. Initial TVC therefore appears to add predictive value only when it reflects the starting abundance of spoilage-associated taxa that later develop under MAP. The late-shelf-life microbiota was relatively stable within each producer, suggesting that consistently selected spoilage-associated taxa may be relevant candidate indicators for future modelling. These findings suggest that adaptive shelf-life determination under MAP is more likely to succeed when based on structured production-day effects, recurrent late-shelf-life microbiota within each producer, and early indicators of spoilage-community development, rather than on initial aerobic TVC alone. Characterising microbiota that are repeatedly selected during refrigerated MAP storage may also support future producer- or facility-level approaches to spoilage prediction and precision food-safety research. However, practical pre-release indicators and prediction models require further validation before implementation.

CRediT authorship contribution statement

Birgitte Moen: Writing – review & editing, Writing – original draft, Visualization, Validation, Supervision, Project administration, Methodology, Investigation, Funding acquisition, Formal analysis, Data curation, Conceptualization. **Beatriz Nunes Silva:** Writing – review & editing, Validation, Methodology, Investigation, Data curation. **Ingrid Måge:** Writing – review & editing, Writing – original draft, Visualization, Validation, Software, Methodology, Formal analysis, Data curation. **Paula Teixeira:** Writing – review & editing, Supervision, Project administration, Methodology. **Solveig Langsrud:** Writing – review & editing, Writing – original draft, Methodology, Funding acquisition, Conceptualization. **Ingunn Berget:** Writing – review & editing, Visualization, Software, Methodology, Formal analysis, Data curation. **Merete Rusås Jensen:** Writing – review & editing, Validation, Methodology, Investigation. **Mari Øvrum Gaarder:** Writing – review & editing, Methodology, Investigation, Data curation. **Ina Aksnes Lian:** Writing – review & editing, Methodology, Investigation. **Dina Fernandes:** Writing – review & editing, Methodology, Investigation. **Solfrid Bjørkøy:** Writing – review & editing, Methodology, Investigation. **Diogo Ferreira:** Writing – review & editing, Methodology, Investigation. **Annette Fagerlund:** Writing – review & editing, Writing – original draft, Supervision, Project administration, Methodology, Funding acquisition, Data curation, Conceptualization.

Declaration of Generative AI and AI-assisted technologies in the writing process

During the preparation of this work the authors used Copilot to refine wording and improve structure. After using this tool, the authors reviewed and edited the content as needed and take full responsibility for the content of the published article.

Declaration of competing interest

The authors declare that they have no known competing financial interests or personal relationships that could have appeared to influence the work reported in this paper.

Acknowledgements

The work was funded by European Union's Horizon Europe research and innovation programme under grant agreement N° 101136248, the Norwegian Fund for Research Fees for Agricultural Products: Micropack (NFR 354136), the Norwegian Fund for Research Fees for Agricultural Products: Enable (NFR 354160) and the Scientific collaboration under the FCT project UID/50016/2025.

Appendix A. Supplementary data

Supplementary data to this article can be found online at https://doi.org/10.1016/j.ijfoodmicro.2026.112066.

Data availability

Data supporting the findings are available in the Supplementary Materials and in the NCBI SRA under BioProject accession PRJNA1310835.

References

Albrecht, A., Ibald, R., Raab, V., Reichstein, W., Haarer, D., Kreyenschmidt, J., 2020. Implementation of time temperature indicators to improve temperature monitoring and support dynamic shelf life in meat supply chains. J. Packag. Technol. Res. 4, 23–32.

Amir, A., McDonald, D., Navas-Molina, J.A., Kopylova, E., Morton, J.T., Xu, Z.Z., Kightley, E.P., Thompson, L.R., Hyde, E.R., Gonzalez, A., Knight, R., 2017. Deblur rapidly resolves single-nucleotide community sequence patterns. mSystems 2, e00191-16.

Bokulich, N.A., Subramanian, S., Faith, J.J., Gevers, D., Gordon, J.I., Knight, R., Mills, D. A., Caporaso, J.G., 2013. Quality-filtering vastly improves diversity estimates from Illumina amplicon sequencing. Nat. Methods 10, 57–59.

Bolyen, E., Rideout, J.R., Dillon, M.R., Bokulich, N., Abnet, C.C., Al-Ghalith, G.A., Alexander, H., Alm, E.J., Arumugam, M., Asnicar, F., Bai, Y., Bisanz, J.E., Bittinger, K., Brejnrod, A., Brislawn, C.J., Brown, C.T., Callahan, B.J., Caraballo-Rodriguez, A.M., Chase, J., Cope, E.K., Da Silva, R., Diener, C., Dorrestein, P.C., Douglas, G.M., Durall, D.M., Duvallet, C., Edwardson, C.F., Ernst, M., Estaki, M., Fouquier, J., Gauglitz, J.M., Gibbons, S.M., Gibson, D.L., Gonzalez, A., Gorlick, K., Guo, J.R., Hillmann, B., Holmes, S., Holste, H., Huttenhower, C., Huttley, G.A., Janssen, S., Jarmusch, A.K., Jiang, L.J., Kaehler, B.D., Bin Kang, K., Keefe, C.R., Keim, P., Kelley, S.T., Knights, D., Koester, I., Kosciolek, T., Kreps, J., Langille, M.G. I., Lee, J., Ley, R., Liu, Y.X., Loftfield, E., Lozupone, C., Maher, M., Marotz, C., Martin, B.D., McDonald, D., McIver, L.J., Melnik, A.V., Metcalf, J.L., Morgan, S.C., Morton, J.T., Naimey, A.T., Navas-Molina, J.A., Nothias, L.F., Orchanian, S.B., Pearson, T., Peoples, S.L., Petras, D., Preuss, M.L., Pruesse, E., Rasmussen, L.B., Rivers, A., Robeson, M.S., Rosenthal, P., Segata, N., Shaffer, M., Shiffer, A., Sinha, R., Song, S.J., Spear, J.R., Swafford, A.D., Thompson, L.R., Torres, P.J., Trinh, P., Tripathi, A., Turnbaugh, P.J., Ul-Hasan, S., van der Hooft, J.J.J., Vargas, F., Vazquez-Baeza, Y., Vogtmann, E., von Hippel, M., Walters, W., Wan, Y.H., Wang, M.X., Warren, J., Weber, K.C., Williamson, C.H.D., Willis, A.D., Xu, Z.Z., Zaneveld, J.R., Zhang, Y.L., Zhu, Q.Y., Knight, R., Caporaso, J.G., 2019. Reproducible, interactive, scalable and extensible microbiome data science using QIIME 2. Nat. Biotechnol. 37, 852–857.

Caporaso, J.G., Lauber, C.L., Walters, W.A., Berg-Lyons, D., Huntley, J., Fierer, N., Owens, S.M., Betley, J., Fraser, L., Bauer, M., Gormley, N., Gilbert, J.A., Smith, G., Knight, R., 2012. Ultra-high-throughput microbial community analysis on the Illumina HiSeq and MiSeq platforms. ISME J. 6, 1621–1624.

Caporaso, J.G., Ackermann, G., Apprill, A., Bauer, M., Berg-Lyons, D., Betley, J., Fierer, N., Fraser, L., Fuhrman, J.A., Gilbert, J.A., Gormley, N., Humphrey, G., Huntley, J., Jansson, J.K., Knight, R., Lauber, C.L., Lozupone, C.A., McNally, S.,

Needham, D.M., Owens, S.M., Parada, A.E., Parsons, R., Smith, G., Thompson, L.R., Thompson, L., Turnbaugh, P.J., Walters, W.A., Weber, L., 2023. EMP 16S Illumina Amplicon Protocol V.2 protocols.io. https://www.protocols.io/view/emp-16s-illumina-amplicon-protocol-kqdg3dzzl25z/v2.

Chen, S.H., Fegan, N., Kocharunchitt, C., Bowman, J.P., Duffy, L.L., 2020. Impact of poultry processing operating parameters on bacterial transmission and persistence on chicken carcasses and their shelf life. Appl. Environ. Microbiol. 86.

Dourou, D., Spyrelli, E.D., Doulgeraki, A.I., Argyri, A.A., Grounta, A., Nychas, G.J.E., Chorianopoulos, N.G., Tassou, C.C., 2021. Microbiota of chicken breast and thigh fillets stored under different refrigeration temperatures assessed by next-generation sequencing. Foods 10.

EC, 2025. EU Agricultural Outlook 2025–2035. European Commission, Directorate-General for Agriculture and Rural Development, Brussels. https://doi.org/10.2762/4491268.

Eurostat, 2025. Poultry Statistics. Statistics Explained. https://ec.europa.eu/eurostat/statistics-explained/index.php?title=Poultry_statistics. (Accessed 20 February 2026).

Gloor, G.B., Macklaim, J.M., Pawlowsky-Glahn, V., Egozcue, J.J., 2017. Microbiome datasets are compositional: and this is not optional. Front. Microbiol. 8, 2224.

Hamady, M., Knight, R., 2009. Microbial community profiling for human microbiome projects: tools, techniques, and challenges. Genome Res. 19, 1141–1152.

Hamady, M., Walker, J.J., Harris, J.K., Gold, N.J., Knight, R., 2008. Error-correcting barcoded primers for pyrosequencing hundreds of samples in multiplex. Nat. Methods 5, 235–237.

Hansen, A.A., Langsrud, S., Carlehög, M., Haugen, J.E., Moen, B., 2023. CO_2 packaging increases shelf life through reduction of off-odor production by CO_2 tolerant bacteria in addition to growth inhibition of the spoilage bacteriota. Food Control 144, 109390.

Hazards, E.P.o.B., Koutsoumanis, K., Allende, A., Alvarez-Ordonez, A., Bolton, D., Bover-Cid, S., Chemaly, M., Davies, R., De Cesare, A., Herman, L., Nauta, M., Peixe, L., Ru, G., Simmons, M., Skandamis, P., Suffredini, E., Jacxsens, L., Skjerdal, T., Da Silva Felicio, M.T., Hempen, M., Messens, W., Lindqvist, R., 2020. Guidance on date marking and related food information: part 1 (date marking). EFSA J. 18, e06306.

Herbert, U., Albrecht, A., Kreyenschmidt, J., 2015. Definition of predictor variables for MAP poultry filets stored under different temperature conditions. Poult. Sci. 94, 424–432.

Holck, A.L., Pettersen, M.K., Moen, M.H., Sorheim, O., 2014. Prolonged shelf life and reduced drip loss of chicken filets by the use of carbon dioxide emitters and modified atmosphere packaging. J. Food Prot. 77, 1133–1141.

Höll, L., Behr, J., Vogel, R.F., 2016. Identification and growth dynamics of meat spoilage microorganisms in modified atmosphere packaged poultry meat by MALDI-TOF MS. Food Microbiol. 60, 84–91.

ICF, Anthesis, Lyndhurst, Brook, WRAP, 2018. Market Study on Date Marking and Other Information Provided on Food Labels and Food Waste Prevention: Final Report. European Commission, Directorate-General for Health and Food Safety. Publications Office of the European Union, Luxembourg. https://doi.org/10.2875/808514.

Jansen, J.J., Hoefsloot, H.C.J., van der Greef, J., Timmerman, M.E., Westerhuis, J.A., Smilde, A.K., 2005. ASCA: analysis of multivariate data obtained from an experimental design. J. Chemometr. 19, 469–481.

Jimenez, S.M., Salsi, M.S., Tiburzi, M.C., Rafaghelli, R.C., Tessi, M.A., Coutaz, V.R., 1997. Spoilage microflora in fresh chicken breast stored at 4 degrees C: influence of packaging methods. J. Appl. Microbiol. 83, 613–618.

Kandeepan, G., Tahseen, A., 2022. Modified atmosphere packaging (MAP) of meat and meat products: a review. J. Packag. Technol. Res. 6, 137–148.

Katiyo, W., de Kock, H.L., Coorey, R., Buys, E.M., 2020. Sensory implications of chicken meat spoilage in relation to microbial and physicochemical characteristics during refrigerated storage. Lwt-Food Sci. Technol. 128, 109468.

Khomich, M., Måge, I., Rud, I., Berget, I., 2021. Analysing microbiome intervention design studies: comparison of alternative multivariate statistical methods. PloS One 16, e0259973.

Kolbeck, S., Ludwig, C., Meng, C., Hilgarth, M., Vogel, R.F., 2020. Comparative proteomics of meat spoilage bacteria predicts drivers for their coexistence on modified atmosphere packaged meat. Front. Microbiol. 11, 209.

Labuza, T., Sam Saguy, I., Taoukis, P., 1997. Kinetics of food deterioration and shelf-life prediction. In: Valentas, K.J., Rotstein, E., Singh, R.P. (Eds.), Handbook of Food Engineering Practice. I CRC Press, pp. 361–404.

Lauritsen, C.V., Kjeldgaard, J., Ingmer, H., Bisgaard, M., Christensen, H., 2019. Microbiota encompassing putative spoilage bacteria in retail packaged broiler meat and commercial broiler abattoir. Int. J. Food Microbiol. 300, 14–21.

Lawless, H.T., Heymann, H., 2010. Sensory Evaluation of Food: Principles and Practices, 2nd ed. Springer, New York.

Lee, H.S., Kwon, M., Heo, S., Kim, M.G., Kim, G.B., 2017. Characterization of the biodiversity of the spoilage microbiota in chicken meat using next generation sequencing and culture dependent approach. Korean J. Food Sci. Anim. Resour. 37, 535–541.

Li, D., Wang, X.J., 2017. Dynamic supply chain decisions based on networked sensor data: an application in the chilled food retail chain. Int. J. Prod. Res. 55, 5127–5141.

Lubbe, S., Filzmoser, P., Templ, M., 2021. Comparison of zero replacement strategies for compositional data with large numbers of zeros. Chemom. Intel. Lab. Syst. 210, 104248.

Marmion, M., Ferone, M.T., Whyte, P., Scannell, A.G.M., 2021. The changing microbiome of poultry meat; from farm to fridge. Food Microbiol. 99, 103823.

McDonald, D., Clemente, J.C., Kuczynski, J., Rideout, J.R., Stombaugh, J., Wendel, D., Wilke, A., Huse, S., Hufnagle, J., Meyer, F., Knight, R., Caporaso, J.G., 2012. The Biological Observation Matrix (BIOM) format or: how I learned to stop worrying and love the ome-ome. Gigascience 1, 7.

Moen, B., Fagerlund, A., Pursti, S.M., Jensen, M.R., Langsrud, S., 2026. Covariation between air chiller and chicken product microbiota in a poultry processing facility. PloS One 21, e0344423.

Morales, P.A., Aguirre, J.S., Troncoso, M.R., Figueroa, G.O., 2016. Phenotypic and genotypic characterization of *Pseudomonas* spp. present in spoiled poultry fillets sold in retail settings. LWT–Food Sci. Technol. 73, 609–614.

Møretrø, T., Langsrud, S., 2017. Residential bacteria on surfaces in the food industry and their implications for food safety and quality. Compr. Rev. Food Sci. Food Saf. 16, 1022–1041.

Møretrø, T., Moen, B., Almli, V.L., Teixeira, P., Ferreira, V.B., Åsli, A.W., Nilsen, C., Langsrud, S., 2021. Dishwashing sponges and brushes: consumer practices and bacterial growth and survival. Int. J. Food Microbiol. 337, 108928.

Naveena, B.M., Khansole, P.S., Kumar, M.S., Krishnaiah, N., Kulkarni, V.V., Deepak, S.J., 2017. Effect of sous vide processing on physicochemical, ultrastructural, microbial and sensory changes in vacuum packaged chicken sausages. Food Sci. Technol. Int. 23, 75–85.

Rognes, T., Flouri, T., Nichols, B., Quince, C., Mahé, F., 2016. VSEARCH: a versatile open source tool for metagenomics. PeerJ 4, e2584.

Rouger, A., Tresse, O., Zagorec, M., 2017. Bacterial contaminants of poultry meat: sources, species, and dynamics. Microorganisms 5, 50.

Rouger, A., Moriceau, N., Prevost, H., Remenant, B., Zagorec, M., 2018. Diversity of bacterial communities in French chicken cuts stored under modified atmosphere packaging. Food Microbiol. 70, 7–16.

Sarfraz, J., Hansen, A.Å., Haugen, J.E., Le, T.A., Nilsen, J., Skaret, J., Huynh, T.P., Pettersen, M.K., 2021. Biodegradable active packaging as an alternative to conventional packaging: a case study with chicken fillets. Foods 10, 1126.

Sequino, G., Cobo-Diaz, J.F., Valentino, V., Tassou, C., Volpe, S., Torrieri, E., Nychas, G.J., Ordóñez, A.A., Ercolini, D., De Filippis, F., 2025. Environmental microbiome mapping in poultry processing chain and assessment of microbial dynamics in response to different storage conditions. Food Microbiol. 128, 104734.

Shao, L.T., Chen, S.S., Wang, H.D., Zhang, J.H., Xu, X.L., Wang, H.H., 2021. Advances in understanding the predominance, phenotypes, and mechanisms of bacteria related to meat spoilage. Trends Food Sci. Technol. 118, 822–832.

Söderqvist, K., Peterson, M., Johansson, M., Olsson, V., Boqvist, S., 2024. A microbiological and sensory evaluation of modified atmosphere-packed (MAP) chicken at use-by date and beyond. Foods 13, 2140.

Spyrelli, E.D., Papachristou, C.K., Nychas, G.E., Panagou, E.Z., 2021. Microbiological quality assessment of chicken thigh fillets using spectroscopic sensors and multivariate data analysis. Foods 10, 2723.

Tarlak, F., 2023. The use of predictive microbiology for the prediction of the shelf life of food products. Foods 12, 4461.

Wang, J.M., Zhuang, H., Hinton, A., Zhang, J.H., 2016. Influence of in-package cold plasma treatment on microbiological shelf life and appearance of fresh chicken breast fillets. Food Microbiol. 60, 142–146.

Zhang, Q.Q., Han, Y.Q., Cao, J.X., Xu, X.L., Zhou, G.H., Zhang, W.Y., 2012. The spoilage of air-packaged broiler meat during storage at normal and fluctuating storage temperatures. Poult. Sci. 91, 208–214.

Zwietering, M.H., Jongenburger, I., Rombouts, F.M., van 't Riet, K., 1990. Modeling of the bacterial growth curve. Appl. Environ. Microbiol. 56, 1875–1881.